

ELECTRONIC SUPPLEMENTARY INFORMATION

to

**Probing the electronic structure of a copper(II) complex with a ligand
derived from a rare metal ion-assisted, crossed-alcohol reaction of
acetone with di-2-pyridyl ketone by cw- and pulse-EPR spectroscopy**

Zoi G. Lada,^{a,b} Yiannis Sanakis,^c Catherine P. Raptopoulou,^c Vassilis Psycharis,^c Spyros P. Perlepes*^{a,b} and George Mitrikas*^c

^aFoundation for Research and Technology- Hellas (FORTH), Institute of Chemical Engineering Sciences (ICE-HT), Platani, P.O. Box 1414, 26504 Patras, Greece.

^bDepartment of Chemistry, University of Patras, 26504 Patras, Greece. E-mail: perlepes@patreas.upatras.gr; Tel: +30 2610 996730

^cInstitute of Nanoscience and Nanotechnology, NCSR "Demokritos", 153 10 Aghia Paraskevi Attikis, Greece. E-mail: g.mitrikas@inn.demokritos.gr; Tel: +30 210 6503304

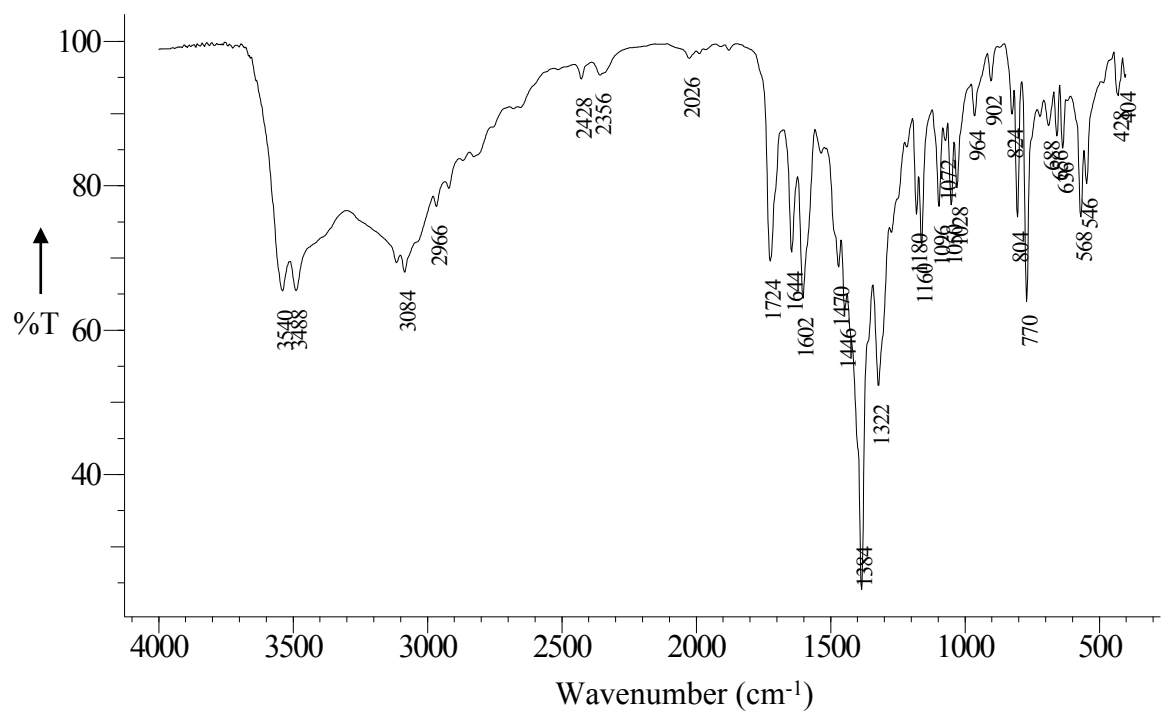


Fig. S1 The IR spectrum (KBr, cm^{-1}) of complex **1**· $2\text{H}_2\text{O}$.

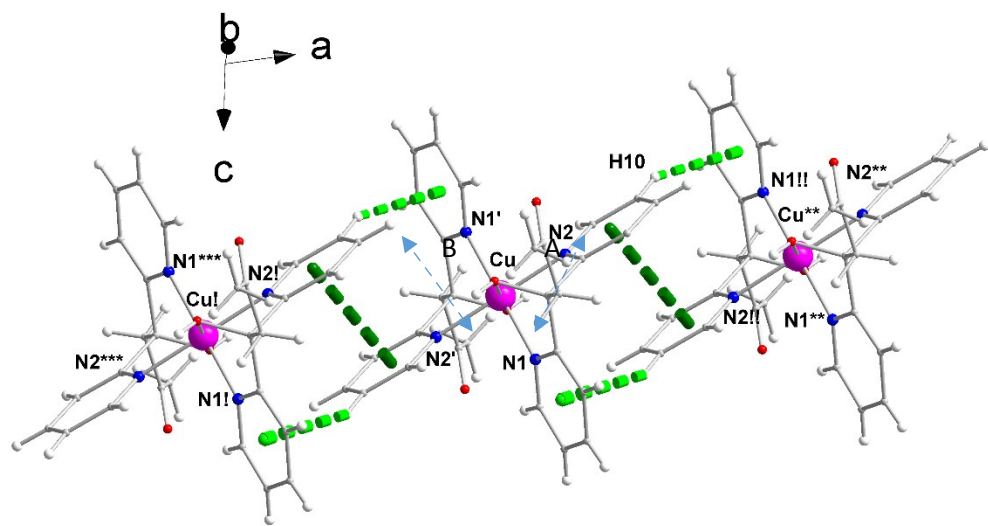


Fig. S2 The communication of the $[\text{Cu}\{(\text{py})_2\text{C}(\text{CH}_2\text{COCH}_3)(\text{OH})\}]^{2+}$ cations through $\text{C}_{\text{aromatic}}\text{-H}\cdots\pi$ and $\pi\cdots\pi$ interactions (dashed light green and dashed dark green lines, respectively) to form chains along the α axis in the crystal structure of complex **1**· $2\text{H}_2\text{O}$. Symmetry codes: (') - $x+1$, - y , - $z+2$; (!) $x-1$, y , z ; (!!) $-x+2$, - y , - $z+2$; (**) $x+1$, y , z ; (****) $-x$, - y , - $z+2$.

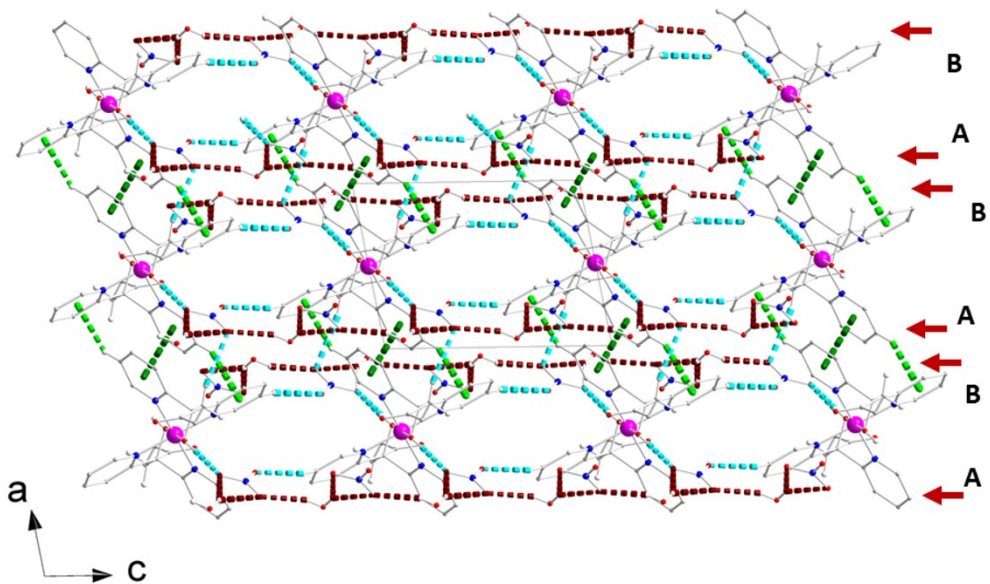


Fig. S3 Layers parallel to the (010) crystallographic plane formed by chains of $[\text{Cu}\{(\text{py})_2\text{C}(\text{CH}_2\text{COCH}_3)(\text{OH})\}_2]^{2+}$ cations along the α axis and chains of $\text{NO}_3^- \cdots \text{H}_2\text{O}$ interactions along the c axis in the crystal structure of **1·2H₂O**. The arrows and the A, B symbols indicate the relative positions (A, above; B, below) of the $\text{NO}_3^- \cdots \text{H}_2\text{O}$ chains with respect to the chains of the cations. Colour codes as in Figs. 4 and S2.

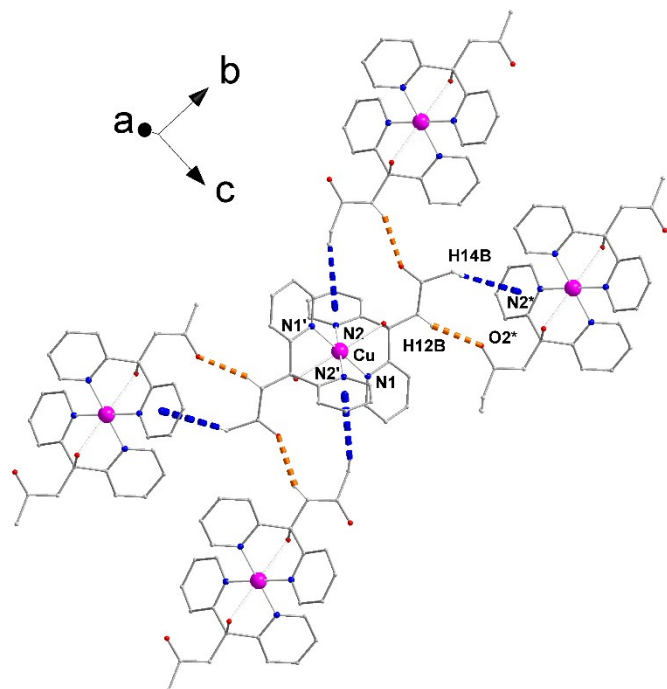


Fig. S4 $\text{C}_{\text{CH}_2}\text{H} \cdots \text{O}_{\text{carbonyl}}$ and $\text{C}_{\text{CH}_3}\text{H} \cdots \pi$ H bonds between $[\text{Cu}\{(\text{py})_2\text{C}(\text{CH}_2\text{COCH}_3)(\text{OH})\}_2]^{2+}$ cations that belong to neighbouring layers stacked along the b axis in the crystal structure of **1·2H₂O**. Orange and blue dashed lines indicate the $\text{C}_{12}\text{H}_{12\text{B}} \cdots \text{O}^{2*}$ and $\text{C}_{14}\text{H}_{14\text{B}} \cdots \text{Cg}^{2*}$ interactions, respectively. Symmetry codes: ('') $-x+1, -y, -z+2$; (*) $x, -y+1/2, z+1/2$.

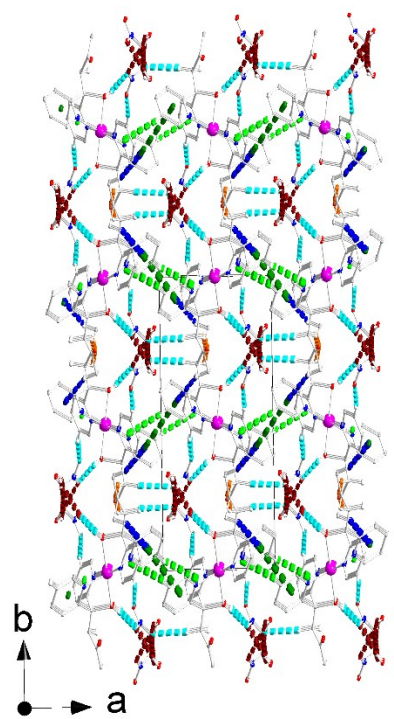


Fig. S5 A portion of the 3D architecture in the crystal structure of **1·2H₂O** as seen along the *c* axis.

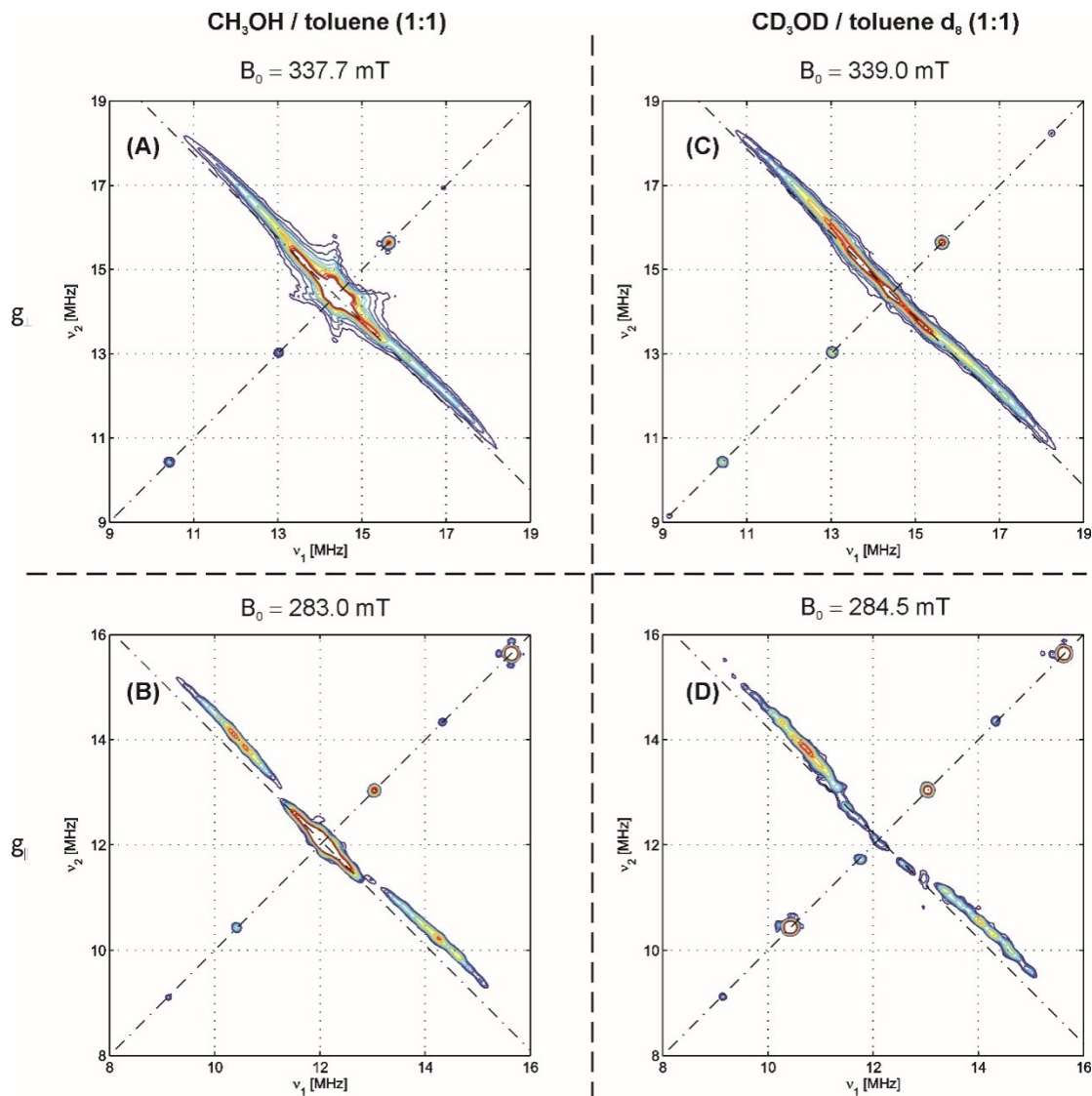


Fig. S6 Comparison of ^1H HYSCORE spectra of **1·2H₂O** measured in normal [(A), (B)] and deuterated [(C), (D)] solvents. The characteristic anisotropic proton hyperfine coupling is present also in the deuterated solvent mixture proving that this signal is attributed to a ligand hydrogen atom.

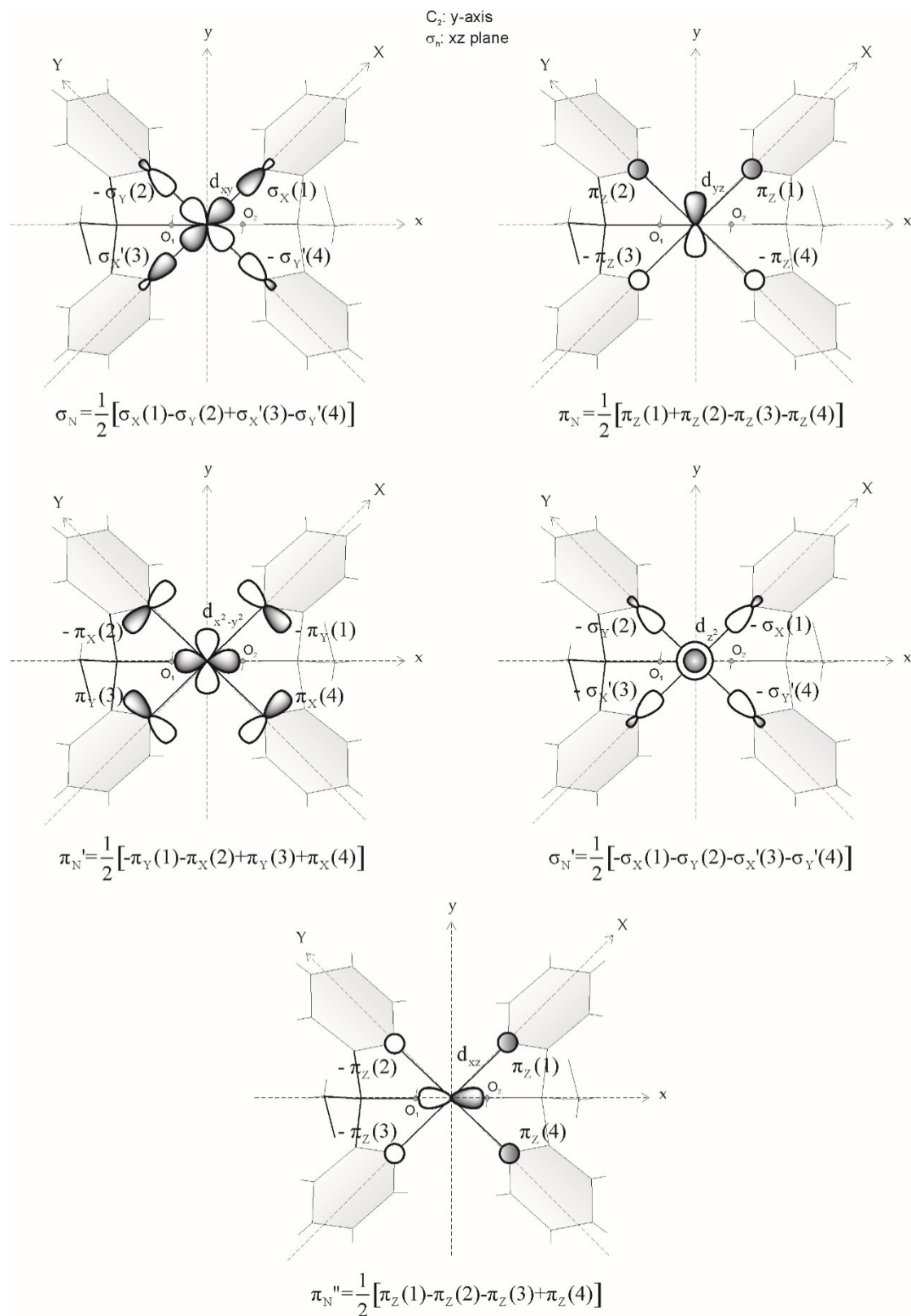


Fig. S7 Schematic representation of the atomic orbitals involved in forming the molecular orbitals described in eqn (8) [main text]. The phase resulting in the antibonding orbitals is not taken into account in this representation.

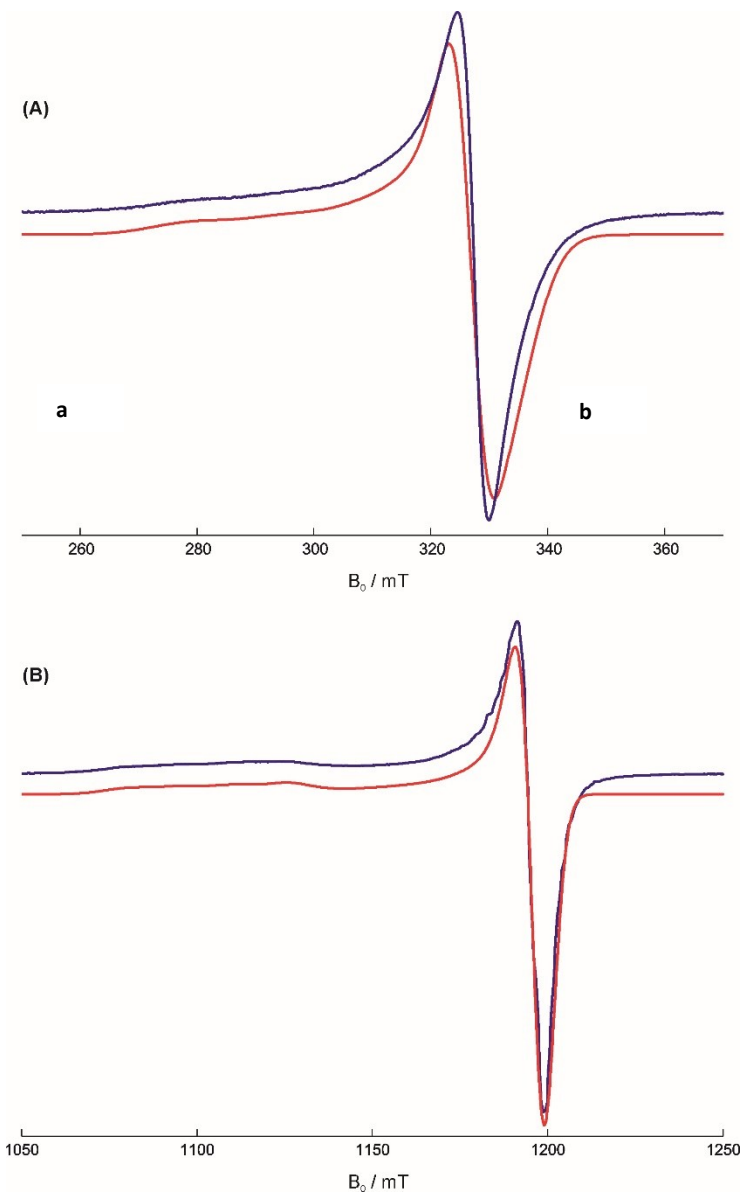


Fig. S8 Solid-state EPR spectra (blue traces) and their simulations (red traces) at room temperature. (A) X-band, $\nu_{\text{mw}}= 9.4328$ GHz; simulation parameters: $(g_x, g_y, g_z)= (2.06, 2.06, 2.23)\pm 0.02$ and $|A_{\perp}|= 20\pm 10$ MHz, $|A_{\parallel}|= 490\pm 40$ MHz. (B) Q-band, $\nu_{\text{mw}}= 34.3587$ GHz; simulation parameters: $(g_x, g_y, g_z)= (2.05, 2.05, 2.23)\pm 0.02$, $|A_{\perp}|= 20\pm 10$ MHz, $|A_{\parallel}|= 470\pm 40$ MHz.

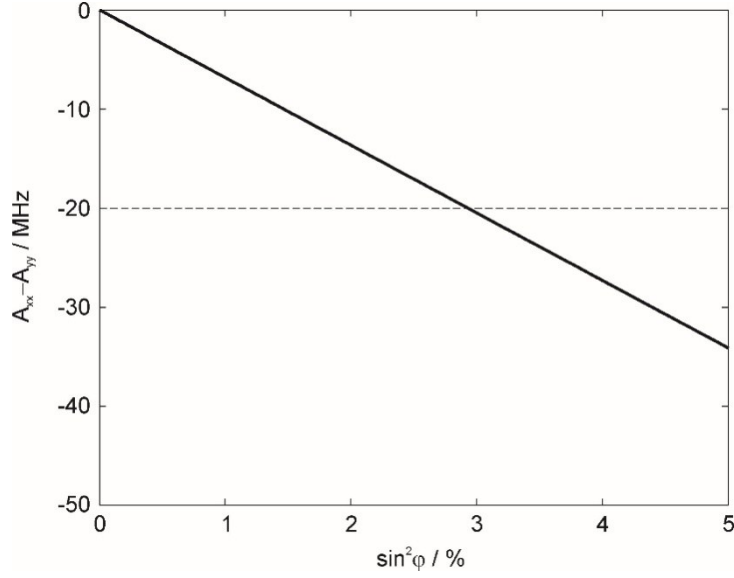


Figure S9 Difference $A_{xx} - A_{yy}$ as a function of the d_{yz} contribution, $\sin^2 \varphi$, calculated using eqn (S3). The dashed line describes the experimentally found maximum difference.

Neglecting ligand atomic orbitals and assuming non-zero mixing only for the ground state $|\Psi_1\rangle$, the g values are given by eqns (S1)⁵⁰

$$\begin{aligned}
 g_{xx} &= g_e + \Delta g_{xx} = 2.0023 + 2\xi\alpha^2 \left[\frac{\varepsilon^2 \cos^2 \varphi}{\Delta_{15}} + \left(\frac{3\gamma^2}{\Delta_{13}} + \frac{\beta^2}{\Delta_{12}} \right) \sin^2 \varphi \right] \\
 g_{yy} &= g_e + \Delta g_{yy} = 2.0023 + 2\xi\alpha^2 \delta^2 / \Delta_{14} \\
 g_{zz} &= g_e + \Delta g_{zz} = 2.0023 + 2\xi\alpha^2 \left(\frac{4\beta^2 \cos^2 \varphi}{\Delta_{12}} + \frac{\varepsilon^2 \sin^2 \varphi}{\Delta_{15}} \right) \\
 g_{xz} &= g_{zx} = -2\xi\alpha^2 \sin \varphi \cos \varphi \left(\frac{2\beta^2}{\Delta_{12}} + \frac{\varepsilon^2}{\Delta_{15}} \right) \\
 g_{xy} &= g_{yx} = g_{yz} = g_{zy} = 0
 \end{aligned} \tag{S1},$$

where $\xi = 830 \text{ cm}^{-1}$ is the Cu^{II} spin-orbit coupling and Δ_{12} , Δ_{13} , Δ_{14} , Δ_{15} denote positive energy differences as shown in Fig. 14b. The ⁶³Cu hyperfine couplings are given by eqns (S2)

$$\begin{aligned}
 A_{xx} &= P \left[-\alpha^2 \kappa + \Delta g_{xx} + \frac{2}{7} \alpha^2 (1 - 3 \sin^2 \varphi) - \frac{3}{7} \xi \alpha^2 \left(\frac{\delta^2}{\Delta_{14}} \cos 2\varphi - \frac{\varepsilon^2}{\Delta_{15}} \sin^2 \varphi \right) \right] \\
 A_{yy} &= P \left[-\alpha^2 \kappa + \Delta g_{yy} + \frac{2}{7} \alpha^2 - \frac{3}{7} \xi \alpha^2 \left(\frac{\varepsilon^2}{\Delta_{15}} + \left(\frac{\gamma^2}{\Delta_{13}} - \frac{\beta^2}{\Delta_{12}} \right) \sin^2 \varphi \right) \right] \\
 A_{zz} &= P \left[-\alpha^2 \kappa + \Delta g_{zz} - \frac{2}{7} \alpha^2 (2 - 3 \sin^2 \varphi) + \right. \\
 &\quad \left. + \frac{3}{7} \xi \alpha^2 \left(\left(\frac{\delta^2}{\Delta_{14}} + \frac{\varepsilon^2}{\Delta_{15}} \right) \cos^2 \varphi - \left(\frac{\beta^2}{\Delta_{12}} + \frac{\delta^2}{\Delta_{14}} - \frac{\gamma^2}{\Delta_{13}} \right) \sin^2 \varphi \right) \right]
 \end{aligned} \tag{S2},$$

$$A_{xz} = P \left[g_{xz} + \frac{6}{7} \alpha^2 \cos \varphi \sin \varphi - \frac{6}{7} \xi \alpha^2 \left(\frac{\beta^2}{\Delta_{12}} - \frac{1}{2} \frac{\varepsilon^2}{\Delta_{15}} + \frac{\delta^2}{\Delta_{14}} \right) \cos \varphi \sin \varphi \right]$$

$$A_{zx} = P \left[g_{zx} + \frac{6}{7} \alpha^2 \cos \varphi \sin \varphi - \frac{6}{7} \xi \alpha^2 \left(\frac{\gamma^2}{\Delta_{13}} - \frac{1}{2} \frac{\varepsilon^2}{\Delta_{15}} + \frac{\delta^2}{\Delta_{14}} \right) \cos \varphi \sin \varphi \right]$$

where $-P\alpha^2\kappa$ is the isotropic hyperfine coupling due to spin polarization and $P = \frac{\mu_0}{4\pi h} g_e g_n^{^{63}\text{Cu}} \beta_e \beta_n \langle r^{-3} \rangle_{3d} = 1171 \text{ MHz}$ is the dipolar hyperfine coupling.⁴⁸ It can be easily seen that for a negligible mixing of the ground state d_{xy} with d_{yz} (*i.e.*, $\sin^2 \varphi \approx 0$), eqns (S1) and (S2) are reduced to the expression for the D_{4h} case⁴⁸ which is the symmetry of the most usual square planar or tetragonally elongated octahedral geometries.

From eqns (S2), we can calculate the difference $A_{xx} - A_{yy}$ as a function of $\sin^2 \varphi$ and the experimentally determined parameters Δg_{xx} , Δg_{yy} and Δg_{zz} . For $\sin^2 \varphi \ll 1$ we get

$$A_{xx} - A_{yy} = P[\Delta g_{xx} - \Delta g_{yy} - \frac{6}{7} \alpha^2 \sin^2 \varphi - \frac{3}{14} \Delta g_{yy} \cos^2 \varphi + \frac{3}{14} \Delta g_{yy} \sin^2 \varphi + \frac{3}{14} \Delta g_{xx} \tan^2 \varphi + \frac{3}{14} \Delta g_{xx} \frac{1}{\cos^2 \varphi} - \frac{1}{14} \Delta g_{zz} \tan^2 \varphi] \quad (\text{S3})$$

Table S1 Numerical values of relevant quantities used in the present work.

Quantity	N(⁴ S)
$\rho_{2s}(0)^a$	4.7687
$\langle r^{-3} \rangle_{2p}^a$	3.0993

^a The values are given in atomic units. Consequently, in order to calculate hyperfine couplings in MHz, the multiplication factor $1/a_0^3 = 6.74833 \times 10^{30} \text{ m}^{-3}$ has to be included in eqns (13)-(15) [main text].

Calculation of Overlap Integrals for Complex 1·2H₂O

$$\begin{aligned} \langle \sigma_N | d_{xy} \rangle &= \frac{1}{2} \langle \sigma_X(1) | d_{xy} \rangle + \frac{1}{2} \langle -\sigma_Y(2) | d_{xy} \rangle + \frac{1}{2} \langle \sigma_X'(3) | d_{xy} \rangle + \frac{1}{2} \langle -\sigma_Y'(4) | d_{xy} \rangle = \\ &= \langle \sigma_X(1) | d_{xy} \rangle + \langle -\sigma_Y(2) | d_{xy} \rangle = \\ &= \sqrt{1-n_N^2} \langle 2s(1) | d_{xy} \rangle + n_N \langle -2p_X(1) | d_{xy} \rangle + \sqrt{1-n_N^2} \langle -2s(2) | d_{xy} \rangle + n_N \langle 2p_Y(2) | d_{xy} \rangle \end{aligned} \quad (\text{S4})$$

$$\begin{aligned}\langle \pi_N | d_{yz} \rangle &= \frac{1}{2} \langle \pi_Z(1) | d_{yz} \rangle + \frac{1}{2} \langle \pi_Z(2) | d_{yz} \rangle + \frac{1}{2} \langle -\pi_Z(3) | d_{yz} \rangle + \frac{1}{2} \langle -\pi_Z(4) | d_{yz} \rangle = \\ &= \langle \pi_Z(1) | d_{yz} \rangle + \langle \pi_Z(2) | d_{yz} \rangle = \langle 2p_Z(1) | d_{yz} \rangle + \langle 2p_Z(2) | d_{yz} \rangle\end{aligned}\quad (\text{S5})$$

$$\langle \pi_N | d_{xy} \rangle = 0 \text{ and } \langle \sigma_N | d_{yz} \rangle = 0 \quad (\text{S6})$$

The necessary overlap integrals between metal and ligand AO used in the present analysis are given in Table S2 for the case where all atoms were considered to be neutral.

Table S2 Overlap integrals of atomic orbitals^a for complex **1**·2H₂O. $R_{N_1,N_2} = 2.013 \text{ \AA}$, $R_{N_2,N_4} = 2.003 \text{ \AA}$.

Group overlap	$\langle \sigma_N d_{xy} \rangle$			$\langle \pi_N d_{yz} \rangle$		
	$ 2s\rangle$	$ -2p_x\rangle$	$ -2s\rangle$	$ 2p_y\rangle$	$ 2p_z\rangle$	$ 2p_z\rangle$
Cu(²S)	N_{1,3}(⁴S)	N_{2,4}(⁴S)	N_{1,3}(⁴S)	N_{2,4}(⁴S)		
$\langle d_{xy} $	0.0759	0.0740	0.0770	0.0746	0	0
$\langle d_{yz} $	0	0	0	0	0.0434	0.0434

^aThe atomic orbitals have been constructed using the expansion coefficients and orbital exponents given in ref. 52 (main text).

Note: References 48 and 50 in the text of the ESI are the same with the corresponding references in the text of main ms.